

## Relationship between spinons and magnetic fields in a fractionalized state

Yu Zhang<sup>1</sup>, Hengdi Zhao<sup>2</sup>, Tristan R. Cao<sup>1</sup>, Rahul Nandkishore<sup>1,3</sup>, Pedro Schlottmann<sup>4</sup>,  
Lance De Long<sup>5</sup>, and Gang Cao<sup>1,6\*</sup>

<sup>1</sup>*Department of Physics, University of Colorado at Boulder, Boulder, CO 80309, USA*

<sup>2</sup>*Materials Science Division, Argonne National Laboratory, Lemont, IL 60439, USA*

<sup>3</sup>*Center for Theory of Quantum Matter, University of Colorado at Boulder, Boulder, CO 80309,  
USA*

<sup>4</sup>*Department of Physics, Florida State University, Tallahassee, FL 32306, USA*

<sup>5</sup>*Department of Physics and Astronomy, University of Kentucky, Lexington, KY 40506, USA*

<sup>6</sup>*Center for Experiments on Quantum Materials, University of Colorado at Boulder, Boulder, CO  
80309, USA*

### ABSTRACT

The 4*d*-electron trimer lattice Ba<sub>4</sub>Nb<sub>1-x</sub>Ru<sub>3+x</sub>O<sub>12</sub> is believed to feature a heavy spinon Fermi surface that underpins both a quantum spin liquid (QSL) and an adjacent heavy-fermion strange metal (HFSM) phase, depending on Nb content. Itinerant spinons act as heat carriers that render the charge-insulating QSL a much better thermal conductor than the HFSM [1]. We find application of magnetic fields up to 14 T below 150 mK induces an abrupt rise in the heat capacity by as much as 5000% and breaks the signature linear temperature dependences of the heat capacity of both phases. In contrast, the AC magnetic susceptibility and the electrical resistivity are insensitive to applied fields up to 14 T over the same milli-Kelvin temperature range, whereas field depresses the thermal conductivity by up to 40% at temperatures below 4 K. These complex phenomena imply applied magnetic field drastically alters the spinons at low temperatures and demand new physics: We propose the steep rise in the heat capacity (and thus entropy) at milli-Kelvin temperatures and strong magnetic fields announces a field-induced localization of spinons.

\*Corresponding author: gang.cao@colorado.edu

Recent experiments [1] indicate that  $\text{Ba}_4\text{Nb}_{1-x}\text{Ru}_{3+x}\text{O}_{12}$  ( $|x| < 0.20$ ) trimer lattices present quantum spin liquid (QSL) physics, strong electron correlations tunable across a metal-to-insulator transition, and a heavy-fermion strange metal (HFSM) phase, as illustrated in **Fig. 1a**. The most striking feature shared by the entire series is the *robust linear-temperature* behavior of the low-temperature heat capacity  $C$  and thermal conductivity  $\kappa$  (as well as the electrical resistivity  $\rho$  for HFSM). These curious behaviors are accompanied by an extraordinarily large Sommerfeld coefficient  $\gamma$  and exchange energy  $\theta_{\text{CW}}$  in the *absence of magnetic order down to 50 mK*, independent of Nb composition and ground state type (**Fig. 1a**). Moreover, the charge-insulating QSL is a much better thermal conductor than the HFSM, and best explained by *charge and spin separation* [1]. The key to these behaviors is a heavy Fermi surface of charge-neutral spinons that provides a *unified framework for describing the entire range of novel phenomena* observed among the  $\text{Ba}_4\text{Nb}_{1-x}\text{Ru}_{3+x}\text{O}_{12}$  trimer lattices and, more broadly, a breakthrough in the ongoing intense effort to study QSL and strange metals [1-8].

Here we report a broad investigation of the  $\text{Ba}_4\text{Nb}_{1-x}\text{Ru}_{3+x}\text{O}_{12}$  ( $|x| < 0.20$ ) trimer lattices that reveals an enigmatic, yet intriguing relationship between spinons and applied magnetic fields  $H$  at milli-Kelvin temperatures  $T$ , which has not been explored before: *Application of  $H$  leads to an abrupt rise in  $C$  by as much as 5000% at the most unlikely conditions of  $T < 150$  mK and  $\mu_0 H = 14$  T. This behavior is inconsistent with existing models and demands novel physics.*

A trimer lattice consisting of three face-sharing metal-oxygen octahedra often behaves unconventionally because the internal degrees of freedom between the three metal ions provide an additional, decisive interaction that generates physical properties that are generally absent in materials with other types of lattices [1, 9-19]. The trimer lattice  $\text{Ba}_4\text{Nb}_{1-x}\text{Ru}_{3+x}\text{O}_{12}$  (**Fig. 1a**) [1, 9, 19] exhibits both the HFSM and the adjacent QSL, depending on Nb concentration  $x$  [1]. The

former corresponds to  $\text{Ba}_4\text{Nb}_{0.81}\text{Ru}_{3.19}\text{O}_{12}$  (“ $\text{Nb}_{0.81}$ ”) and the latter  $\text{Ba}_4\text{Nb}_{1.16}\text{Ru}_{2.84}\text{O}_{12}$  or (“ $\text{Nb}_{1.16}$ ”) (**Fig. 1a**) [19].

The anomalous sensitivity of  $C$  and itinerant spinons to  $H$  at milli-Kev temperatures  $T$  is an observation of central importance to this work. We first focus on  $C$  for 50 mK – 1 K at  $\mu_0H = 0$  and 14 T for both HFSM and QSL phases (**Fig. 1b-c**). As already established [1], for  $\mu_0H = 0$  T, a linear  $C(T)$  is persistent down to 50 mK with a large  $\gamma \leq 240$  mJ/mole  $\text{K}^2$  (**Fig. 1b-c**). However, for  $\mu_0H = 14$  T,  $C$  rises rapidly below an onset temperature  $T_S = 150$  mK for both phases (**Fig. 1b-c**). The field-induced increase in  $C$ , defined by  $\Delta C/C(0) = [C(H) - C(0)]/C(0)$ , can reach as high as 5000% at 50 mK (**Fig. 2a-2b**). This represents a huge entropy enhancement below  $T_S$ , and strikingly contradicts the conventional wisdom that a strong  $H$  (e.g., 14 T) coupled with low  $T$  (e.g., 50 mK) should strongly depress entropy by promoting order that reduces internal energy. In sharp contrast with  $C$  (**Fig. 1b-c**), both the  $a$ -axis AC magnetic susceptibility  $\chi_a'$  of the QSL and  $a$ -axis resistivity  $\rho_a$  of the HFSM measured over the same  $T$  range display only *weak, featureless responses* to the application of 14 T (**Fig. 2c-2d**).

We note that  $\Delta C$  is independent of the orientation of  $H$  for both HFSM and QSL, as evidenced in  $C(T)$  for  $\mu_0H = 14$  T (**Fig. 1b-1c**) and  $C(H)$  at  $T = 100$  mK (**Fig. 2e**). The lack of field anisotropy indicates an absence of orbital coupling and the importance of the Zeeman interaction in coupling relevant degrees of freedom to  $H$ , and further highlights the nature of spinons as fractional excitations. In contrast, both  $\rho_a$  and  $\rho_c$  at 5 K for the QSL are a strong function of field-orientation, and exhibit a pronounced oscillatory behavior with as a function of the angle between  $H$  and the applied current  $I$  (**Fig. S1**) [19, 20 and references therein].

For comparison,  $C(T,H)$  data of a related trimer metal, 9R-BaRuO<sub>3</sub>, and insulating Nb<sub>2</sub>O<sub>5</sub> are also shown in **Fig. 1d** and **Fig. 2f** under the same conditions. Both the  $T$ - and  $H$ -dependences

of  $C$  exhibit no similarities to those of the HFSM and QSL, which decisively eliminates any possible spurious effects from the Ba, Ru, and Nb starting materials and/or contributions from their nuclear heat capacities. Therefore, the observed  $\Delta C$  anomalies must be unique to  $\text{Ba}_4\text{Nb}_{1-x}\text{Ru}_{3+x}\text{O}_{12}$ .

We also explored whether the field-induced rise in  $C$  (**Figs. 1b-c**) could be due to a Schottky effect caused by a splitting  $\delta$  between two levels: Consider the high- $T$  tail of a Schottky peak located well below 50 mK, which would not be fully accessible to experiment unless  $H$  increases  $\delta$ , which would shift the Schottky peak to higher  $T$ . Note the high- $T$  shoulder of the Schottky contribution for  $T \gg \delta$  is proportional to  $DT^{-2}$  ( $D$  = Schottky coefficient), and possibly observable. Combining  $DT^{-2}$  with a  $\gamma T$  contribution due to spinons yields a total  $C = \gamma T + DT^{-2}$  that adequately describes both phases for  $50 \text{ mK} \leq T \leq 1 \text{ K}$  in the presence of  $H$ . Fitting  $C(T, 14T)$  to  $C/T = \gamma + DT^{-3}$  determines values of  $D$  for both phases at  $\mu_0 H = 14 \text{ T}$  (**Fig. 3a**).

It is important that the observed  $C = \gamma T$  over  $50 \text{ mK} \leq T \leq 8 \text{ K}$  at  $H = 0$  (**Figs. 1b-1c** and [1]), which demands that *the phonon (Debye) contribution to  $C$  ( $\sim T^3$ ) is either zero or negligible*. A few additional features are worth noting: (1) The  $D$  values for both phases are essentially identical, *suggesting that the degrees of freedom responsible for  $\Delta C$  are the same*. (2) The magnitude of the  $D$  values,  $10^{-3} \text{ JK/mole}$ , is three orders of magnitude greater than that,  $10^{-6} \text{ JK/mole}$ , due to the quadrupolar and/or magnetic spin splittings of Ru nuclei [21], strongly indicating that the ‘‘Schottky anomaly’’ is *not of nuclear origin*. Furthermore, a conventional Schottky peak rapidly shifts to higher  $T$  with increasing  $H$  that widens the splitting; however, this behavior is not evident (**Figs. 3c-3d**), and  $C(H, T)$  roughly scales with  $H^2$  below 200 mK (**Fig. 3b**).

For comparison, similar measurements were conducted for a 2.5% Pr-doped, isostructural  $\text{Ba}_4\text{Nb}_{1-x}\text{Ru}_{3+x}\text{O}_{12}$  trimer in which the Pr doping introduces a conventional electronic Schottky

anomaly characterized by an upturn in  $C(T,H)$  at  $H = 0$  below 200 mK (**Fig. 3e**). As expected, the Pr Schottky anomaly rapidly shifts to higher  $T$  with increasing  $H$ , in sharp contrast with the behavior of the HFSM and QSL in **Figs. 3c-3d**. In sum, the data in **Fig. 3** suggest that a conventional Schottky effect alone does not provide an adequate explanation of the  $\Delta C(H)$  data for  $T < T_S = 150$  mK.

We now turn to the thermal conductivity  $\kappa$  measured over the range 1.7 K – 10 K at selected  $H$ . It is established that both phases are dominated by spinons at low  $T$  [1]. What is intriguing is that  $H$  readily suppresses  $\kappa$  in both phases (**Figs. 4a-4b**), which is inconsistent with experimental precedents [e.g., 22, 23, 24, 25, 26]. That is,  $\kappa$  is typically proportional to  $C$ , the velocity  $v$  of heat carriers and the mean free path  $l$  of the heat carriers (i.e.,  $\kappa \sim Cv l$ ). Since  $v$  and  $l$  are essentially constant at low  $T$  [27],  $C$  is expected to dictate  $\kappa$ . In the present case, since  $C$  does not change with  $H$  over the range, 1.7 K – 10 K (**Figs. 4d-4e**), the reduction of  $\kappa$  indicates a significant reduction of the spinon velocity  $v$  due to  $H$ . The magnetic field effect on the  $a$ -axis  $\kappa_a$  is strong when  $H$  initially increases from 0 T to 7 T but becomes weaker with further increases from 7 T to 14 T, suggesting a trend toward saturation with increasing  $H$  (**Fig. 4a**).

A close examination of **Figs. 4a-4b** reveals that the field effect on  $\kappa_a$  is a strong function of  $T$  below 4 K, so we introduce a magneto-thermal-conductivity ratio, defined by  $\Delta\kappa_a/\kappa_a(0T) = [\kappa_a(14T) - \kappa_a(0T)]/\kappa_a(0T)$ , to quantify the reduction in  $\kappa_a$  due to application of 14 T. Note that  $\Delta\kappa_a$  reflects contributions from heat carriers that are sensitive to  $H$ . Since the QSL is a charge insulator,  $\Delta\kappa_a$  must be due primarily to spinons at low  $T$  (*note that a typical phonon contribution to  $\kappa$  ( $\sim T^3$ ) is not apparent below 8 K where both  $\kappa$  and  $C$  vary linearly with  $T$  (**Figs. 1b-1c, 4a-4b** and [1]).*  $\Delta\kappa_a/\kappa_a(0T)$  for both phases exhibits a rapid downturn for  $T < 4$  K, resulting in a swift reduction of  $\kappa_a$  by as much as 40% near 1.7 K (**Fig. 4c**). Because  $C$  in the same  $T$  range

remains unchanged (**Figs. 4d-4e**), the increasingly negative  $\Delta\kappa_a/\kappa_a(0T)$  with decreasing  $T$  (**Fig. 4c**) strongly indicates that the mobility of spinons must decrease rapidly with decreasing  $T$  as a result of  $H$ . At this rate of the deceleration of spinons, it is conceivable that a strong  $H$  such as 14 T could eventually localize otherwise itinerant spinons as  $T \rightarrow 0$ . This point is schematically illustrated in **Fig. 4f** [19]. Note that the absolute values of both  $\Delta\kappa_a/\kappa_a(0T)$  (**Fig. 4c**) and  $\Delta C/C(0)$  (**Figs. 2a-2b**) are greater in the QSL than in the HFSM, which is consistent with there being more spinons in the QSL than in the HFSM.

Here we discuss possible explanations. We start by noting that  $C$  is independent of field orientation (**Figs. 1b-1c, Fig.2e**), which strongly indicates that the relevant degrees of freedom that drive  $\Delta C$  must couple to  $H$  only through the Zeeman interaction, and not through the orbital coupling. That is,  $C$  below  $T_s = 150$  mK is dominated by spinful degrees of freedom which are either immobile or charge neutral (or both) in response to  $H$ . The obvious candidates are charge-neutral spinons [1] that dominate  $C$  and  $\kappa$  in both the HFSM and QSL. Furthermore, the qualitatively similar behavior of  $C$  in both phases (**Figs. 1b-1c**) indicates nothing special happens to the spinons at the metal-insulator transition, consistent with [1].

It remains to explain the steep upturn in  $C$  at  $T < T_s (= 150$  mK) and  $\mu_0 H = 14$  T (**Figs. 1b-1c**)? *Prima facie*, the  $C \propto H^2/T^2$  scaling for  $T = 50$ -200 mK (**Fig. 3b**) suggests that the rapid upturn in  $C$  might be the high- $T$  tail of a ‘Schottky anomaly’, as discussed above, where the level splitting  $\delta$  in question arises from a Zeeman splitting of the valence electron states, as nuclear spins would produce an anomaly three orders of magnitude too weak (**Fig. 3a**) [21]. Moreover, core electron states can be ruled out by the absence of any corresponding anomaly in BaRuO<sub>3</sub> and Nb<sub>2</sub>O<sub>5</sub> (**Figs. 1d, 2f**). Noting  $\rho_a$  and  $\chi_a$  exhibit no corresponding anomaly (**Figs. 2c-2d**) is observed under the same conditions further confirms the sharp rise in  $C$  is not associated with a magnetic or

electronic phase transition. A reasonable working hypothesis is that the abrupt rise in  $C$  is due to a novel *charge-neutral spinon Schottky anomaly* common to both the QSL and HFSM.

The above interpretation must address a broader set of questions: **(1)** If the spinons are itinerant and dominate  $\kappa$  in the absence of  $H$  [1], how do they form two-level systems and give rise to a Schottky anomaly? **(2)** Why does the upturn in  $C$  only manifest itself at  $T < T_S$  (**Figs. 1b-1c**)? **(3)** Why does the presence or absence of the upturn in  $C$  essentially depend on the *presence or absence* of  $H$  but less so on the *strength* of  $H$  (see **Fig. 3d**), whereas in traditional Schottky systems the onset sensitively depends on the strength of  $H$  (**Fig. 3e**)?

A crucial clue comes from the data for  $\kappa_a$  which indicates that the spinon mobility decreases in the presence of  $H$ , and this decrease accelerates at  $T < 4$  K, giving rise to the increasingly negative  $\Delta\kappa_a/\kappa_a(0T)$  (**Fig. 4c**). This suggests that the spinons are itinerant in the absence of  $H$ , but less so in the presence of  $H$ , and may eventually become localized below  $T_S$  for  $\mu_0H = 14$  T. We propose that the upturn in  $C$  arises only when spinons are localized and form two-level systems. We therefore posit  $T_S$  marks the onset of localization (or a ‘mobility gap’) of the spinons in the presence of  $H$  (this explains points (1) and (2)).

It remains to explain as to why the spinon Schottky anomaly manifests itself only in the presence of  $H$ , and yet its onset at  $T_S$  is less sensitive to the strength of  $H$ , compared to that of the conventional Schottky anomaly (**Figs. 3c-3e**). This may be explained if the zero-field spinon system is in the symplectic symmetry class and, being quasi-two dimensional, experiences weak antilocalization [28]. Applying  $H$  would then change the symmetry class, destroying weak antilocalization and opening the door to Anderson localization at low  $T$ . Once the spinons localize, two-level systems appear. In other words, the main role of  $H$  is to change the symmetry class and enable localization, so the presence or absence of  $H$  matters, but the strength of  $H$  is less important.

This explanation neatly resolves the point (3) and is consistent with the H-reduced  $\kappa_a$  (**Fig. 4**). We note a well-studied impurity model with similar properties to this spinon system is the overcompensated multichannel Kondo problem [29]. Some results are summarized in [19].

It thus appears that a minimal explanation for all the experimental observations is that ***C is dominated by spinons in both the QSL and HFSM.*** In the absence of H, the spinons are itinerant down to milli-Kelvin temperatures due to weak antilocalization physics. Application of H changes the symmetry class, destroying antilocalization, opening the door to Anderson localization of spinons below  $T_s = 150$  mK, as schematically shown in **Fig. 4g**. Once the spinons localize, they form two-level systems, with a Zeeman splitting proportional to H, and this produces a sharp spinon Schottky anomaly in C (**Figs. 1c-1d**).

We have assumed that localized and itinerant spinons do not co-exist, consistent with current wisdom, but recent theoretical investigations [8, 30] have raised the possibility of excitations with ‘fractionalized’ mobility (aka ‘fractons’). One could thus invoke a more exotic explanation, wherein  $\Delta C$  comes from immobile spin ‘fracton’ excitations, which pair to form itinerant spinon composites that dominate  $\kappa$  in the absence of H. The main role of H in this scenario would be to separate the mobile spinon composites into the immobile ‘fracton’ excitations. However, it would then be necessary to explain why the ‘field-induced unbinding’ only happens below  $T_s$ , which does not have an obvious explanation, and therefore seems a less natural explanation compared to spinon localization.

In summary, this work reveals an extraordinary sensitivity of C and spinons to a strong H at milli-Kelvin temperatures. This behavior is not consistent with any existing models and demands novel physics.



**ACKNOWLEDGEMENTS** G.C. thanks Feng Ye, Xi Dai, Tai-Kai Ng, Sandeep Sharma, Minhyea Lee and Longji Cui for useful discussions. Experimental work is supported by National Science Foundation via Grant No. DMR 2204811. Theoretical work by R.N. was supported by the U.S. Department of Energy (DOE), Office of Science, Basic Energy Sciences (BES) under Award # DE-SC0021346.

## **REFERENCES**

1. Hengdi Zhao, Yu Zhang, Pedro Schlottmann, Lance DeLong, Rahul Nandkishore and Gang Cao, Transition between heavy-fermion-strange-metal and spin liquid in a 4d-electron trimer lattice, *Phys. Rev. Lett.* **132**, 226503 (2024)
2. P. W. Anderson, Resonating valence bonds: a new kind of insulator? *Mater. Res. Bull.* **8**, 153–160 (1973)
3. P.W. Anderson, The resonating valence bond state in  $\text{La}_2\text{CuO}_4$  and superconductivity, *Science* **235**, 1196 (1987)
4. P. A. Lee, An End to the Drought of Quantum Spin Liquids, *Science* **321**, 1306-1307 (2008)
5. L. Savary, L. Balents, Quantum spin liquids: A review, *Rep. Prog. Phys.* **80**, 016502 (2017).
6. Y. Zhou, K. Kanoda, T.-K. Ng, Quantum spin liquid states, *Rev. Mod. Phys.* **89**, 025003 (2017).
7. C. Broholm, R. Cava, S. Kivelson, D. Nocera, M. Norman, T. Senthil, Quantum spin liquids, *Science* **367**, 263 (2020)
8. Rahul M. Nandkishore and Michael Hermele, Fractons, *Annu. Rev. Condens. Matter Phys.* **10**, 295 (2019).
9. L. T. Nguyen, T. Halloran, W. Xie, T. Kong, C. L. Broholm, and R. J. Cava, Geometrically frustrated trimer-based Mott insulator, *Phys. Rev. Mater.* **2**, 054414 (2018)

10. L. T. Nguyen and R. J. Cava, Trimer-based spin liquid candidate  $\text{Ba}_4\text{NbIr}_3\text{O}_{12}$ , *Phys. Rev. Materials* **3**, 014412 (2019).
11. L. T. Nguyen and R. J. Cava, Hexagonal Perovskites as Quantum Materials, *Chem. Rev.* **121**, 2935 (2021)
12. S. V. Streltsov and D. I. Khomskii, Cluster Magnetism of  $\text{Ba}_4\text{NbMn}_3\text{O}_{12}$ : Localized Electrons or Molecular Orbitals, *JETP Lett.* **108**, 686 (2018).
13. Evgenia V. Komleva , Daniel I. Khomskii, and Sergey V. Streltsov, Three-site transition-metal clusters: Going from localized electrons to molecular orbitals, *Phys. Rev. B* **102**, 174448 (2020)
14. G. Cao, H. D. Zhao, H. Zheng, Y. F. Ni, Christopher. A. Pocs, Y. Zhang, Feng, Ye, Christina Hoffmann, Xiaoping Wang, Minhyea Lee, Michael Hermele and Itamar Kimchi, Quantum liquid from strange frustration in the trimer magnet  $\text{Ba}_4\text{Ir}_3\text{O}_{10}$ , *npj Quantum Materials* **5**, 26 (2020)
15. Y. Shen, J. Sears, G. Fabbris, A. Weichselbaum, W. Yin, H. Zhao, D. G. Mazzone, H. Miao, M. H. Upton, D. Casa, R. S. Acevedo-Esteves, C. Nelson, A. M. Barbour, C. Mazzoli, G. Cao, and M. P. M. Dean, Emergence of spinons in layered trimer iridate  $\text{Ba}_4\text{Ir}_3\text{O}_{10}$ , *Phys. Rev. Lett.* **129**, 207201 (2022)
16. A. Sokolik, S. Hakani, S. Roy Susmita, N. Pellatz, H. Zhao, G. Cao, I. Kimchi, D. Reznik, Spinons and damped phonons in spin-1/2 quantum-liquid  $\text{Ba}_4\text{Ir}_3\text{O}_{10}$  observed by Raman scattering, *Phys. Rev. B* **106**, 075108 (2022)
17. Yu Zhang, Yifei Ni, Hengdi Zhao, Sami Hakani, Feng Ye, Lance DeLong, Itamar Kimchi, and Gang Cao, Control of chiral orbital currents in a colossal magnetoresistance material, *Nature* **611**, 467 (2022)

18. Yu Zhang, Yifei Ni, Pedro Schlottmann, Rahul Nandkishore, Lance DeLong and Gang Cao, Current-sensitive Hall effect in a chiral-orbital-current state. *Nat Commun* **15**, 3579 (2024)
19. Supplemental Material
20. L. B. Ioffe, B. Z. Spivak, Giant magnetoresistance in the variable-range hopping regime. *J. Exp. Theor. Phys.* **117**, 551–569 (2013)
21. Z. X. Zhou, S. McCall, C.S. Alexander, J.E. Crow, P. Schlottmann, A. Bianchi, C. Capan, R. Movshovich, K.H. Kim, M. Jaime, and N. Harrison, M. Haas, R. Cava and G. Cao, Transport and thermodynamic properties of  $\text{Sr}_3\text{Ru}_2\text{O}_7$  near the quantum critical point, *Phys. Rev. B* **69**, 140409 (2004)
22. Ian A. Leahy, Christopher A. Pocs, Peter E. Siegfried, David Graf, S.-H. Do, Kwang-Yong Choi, B. Normand, and Minhyea Lee, Anomalous Thermal Conductivity and Magnetic Torque Response in the Honeycomb Magnet  $\alpha\text{-RuCl}_3$ , *Phys. Rev. Lett.* **118**, 187203 (2017)
23. P. Czajka, T. Gao, M. Hirschberger, *et al.* Oscillations of the thermal conductivity in the spin-liquid state of  $\alpha\text{-RuCl}_3$ . *Nat. Phys.* **17**, 915–919 (2021)
24. J F Gregg and D ter Haar, On the effect of a magnetic field on the thermal conductivity, *Eur. J. Phys.* **17** 303 (1996)
25. Rajasree Das, Amit Chanda and Ramanathan Mahendiran, Influence of magnetic field on electrical and thermal transport in the hole doped ferromagnetic manganite:  $\text{La}_{0.9}\text{Na}_{0.1}\text{MnO}_3$ , *RSC Adv.* **9**, 1726 (2019)
26. N. Wakeham, A. Bangura, X. Xu, *et al.* Gross violation of the Wiedemann–Franz law in a quasi-one-dimensional conductor. *Nat Commun* **2**, 396 (2011)

27. F. Steckel, A. Matsumoto, T. Takayama, H. Takagi, B. Buchner and C. Hess, Pseudospin transport in the  $J_{\text{eff}} = 1/2$  antiferromagnet  $\text{Sr}_2\text{IrO}_4$ , *EPL* **114** 57007 (2016)
28. S. Hikami, A.I. Larkin and Y. Nagaoka, Spin-orbit interaction and magnetoresistance in the two dimensional random system, *Progress of Theoretical Physics* **63**, 2, 707 (1980)
29. P. Schlottmann and P.D. Sacramento, Multichannel Kondo problem and some applications, *Advances in Physics* **42**, 641 (1993)
30. A. Gromov and L. Radzihovsky, *Colloquium: Fracton matter*, *Rev. Mod. Phys.* **96**, 011001 (2024)

#### FIGURE LENGENDS

**Fig. 1. Phase diagram and key features.** **a**, A schematic phase diagram for the heavy spinon fermi surface featuring the extraordinarily large Sommerfeld coefficient  $\gamma$  (blue) and exchange energy  $\theta_{\text{CW}}$  (red, right scale) as a function of Nb content  $x$  for the entire  $\text{Ba}_4\text{Nb}_{1-x}\text{Ru}_{3+x}\text{O}_{12}$  series [1]. Inset: The crystal structure of the trimer lattice. Note that the heavy-fermion strange metal (HFSM,  $1-x = 0.81$  or  $\text{Nb}_{0.81}$ ) and the insulating quantum spin liquid (QSL,  $1-x = 1.16$  or  $\text{Nb}_{1.16}$ ) are adjacent to each other. The heat capacity  $C(T)$  for  $50 \text{ mK} \leq T \leq 1 \text{ K}$  at magnetic fields  $\mu_0 H = 0$  and  $14 \text{ T}$  for **b**, the HFSM, and **c**, the QSL for both  $H \parallel a$  axis and  $H \parallel c$  axis. The black arrows mark the onset of the upturn in  $C$ . **d**,  $C(T)$  for  $9\text{R-BaRuO}_3$  (solid circles and lines) and  $\text{Nb}_2\text{O}_5$  (lines) culled at the same conditions for comparison; note that  $C$  behaves normally, without any upturn at  $14 \text{ T}$  observed in the HFSM and QSL.

**Fig. 2. Physical properties of the HFSM and QSL.** The  $H$ -dependence of  $[C(H) - C(0)]/C(0)$  at selected  $T$  for **a**, the QSL and **b**, the HFSM. The  $T$ -dependence for  $50 \text{ mK} \leq T \leq 1 \text{ K}$  of **c**, the  $a$ -axis  $\rho_a$  for HFSM, **d**, the  $a$ -axis AC susceptibility  $\chi'_a$  for the QSL at representative  $H$ . The  $H$ -dependence at  $T = 100 \text{ mK}$  and up to  $\mu_0 H = 14 \text{ T}$  of  $C$  for **e**, the QSL for both  $H \parallel a$  axis and  $H \parallel c$  axis, and **f**,  $\text{BaRuO}_3$  for  $H \parallel c$  axis for comparison. Note  $C(H)$  for the QSL is independent of the orientation of  $H$ .

**Fig. 3. The Schottky-like effect.** **a**,  $C/T$  vs.  $1/T^3$  for  $50 \text{ mK} \leq T \leq 1 \text{ K}$  for both the HFSM and QSL. Note the slope  $D$  ( $\sim 10^{-3} \text{ JK/mole}$ ) for both phases is essentially the same, and three orders

of magnitude larger than that due to the quadrupolar and/or magnetic spin splitting of Ru nuclei. **b**,  $C$  as a function of  $H^2$  at representative  $T$  for the QLS. **c**,  $C(T)$  for  $50 \text{ mK} \leq T \leq 600 \text{ mK}$  as a function of  $T$  at selected  $H$  for **c**, the HFSM, **d**, the QLS, and **e**,  $\text{Ba}_{3.90}\text{Pr}_{0.10}\text{Nb}_{0.84}\text{Ru}_{3.16}\text{O}_{12}$  for comparison; the black arrows are a guide to the eye. Note the distinct differences in the sensitivity and the sharpness of the upturn in  $C$  between the compounds.

**Fig. 4. Thermal conductivity  $\kappa$  at magnetic fields.** The  $T$ -dependence for  $1.7 \text{ T} \leq T \leq 10 \text{ K}$  of the  $a$ -axis  $\kappa_a$  at representative  $H$  for **a**, the QLS, and **b**, the HFSM. Note the same scale of  $\kappa_a$  in **a** and **b** and the significant suppression of  $\kappa_a$  due to  $H$ . **c**,  $\Delta\kappa_a/\kappa_a(0T)$  as a function of  $T$  for the QLS and HFSM where  $\Delta\kappa_a = \kappa_a(14T) - \kappa_a(0T)$ . Note the rapid drop in  $\Delta\kappa_a/\kappa_a(0T)$  as  $T \rightarrow 0$ .  $C(T)$  for the same  $T$  range at  $\mu_0H = 0$  and  $14 \text{ T}$  for **d**, the QSL and **e**, HFSM. Note that  $C(T)$  remains essentially unchanged at  $14 \text{ T}$ . **f**, Schematic illustrating the spinons (green dots) as heat carriers at  $H = 0$  and  $H \neq 0$  and that  $H$  reduces the spinon velocity  $v$  at  $T > T_s$  and destroys it, localizing the spinons at  $T < T_s$ . **g**, Schematic  $T$ - $H$  phase diagram for the spinons at low  $T$ .

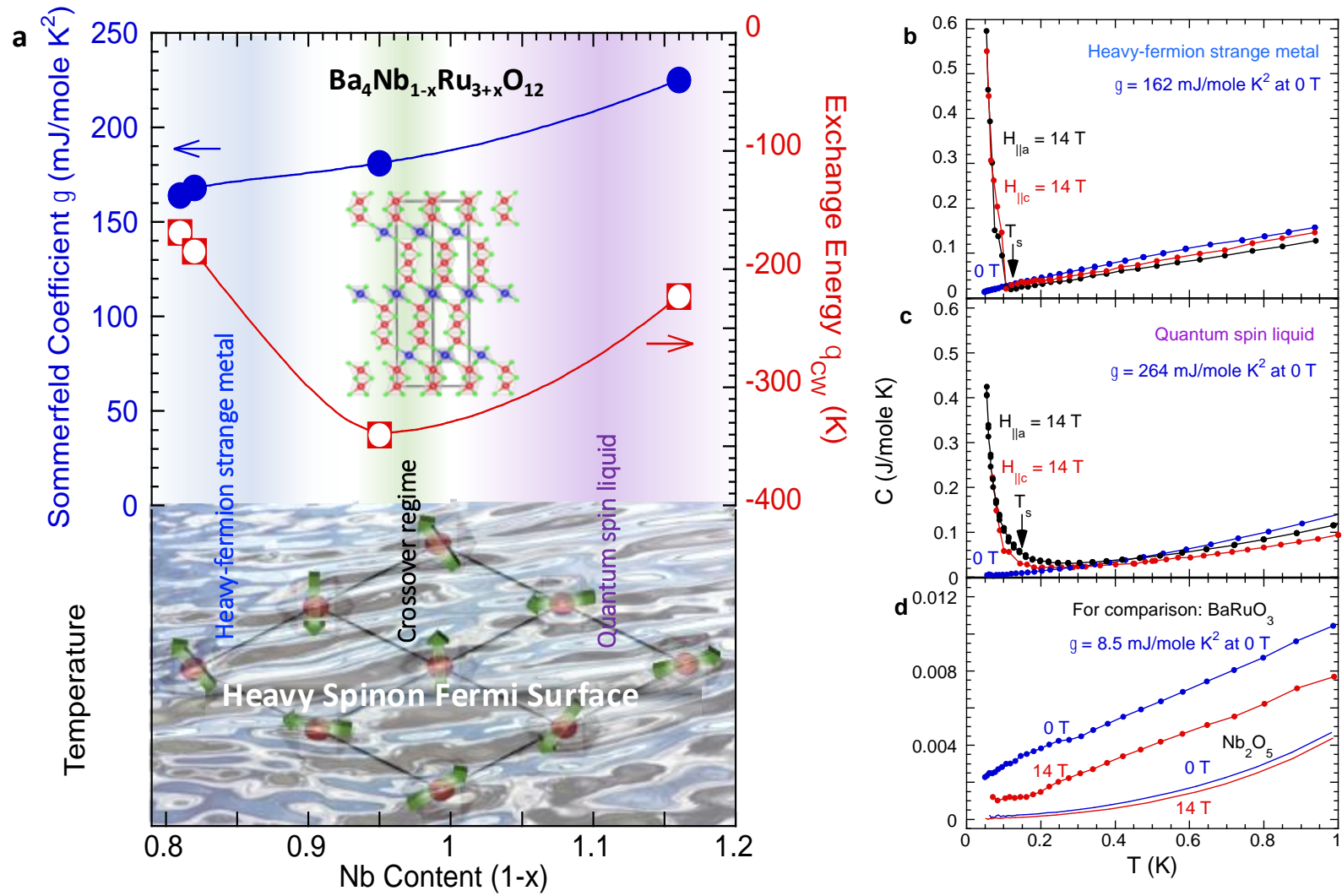


Figure 1

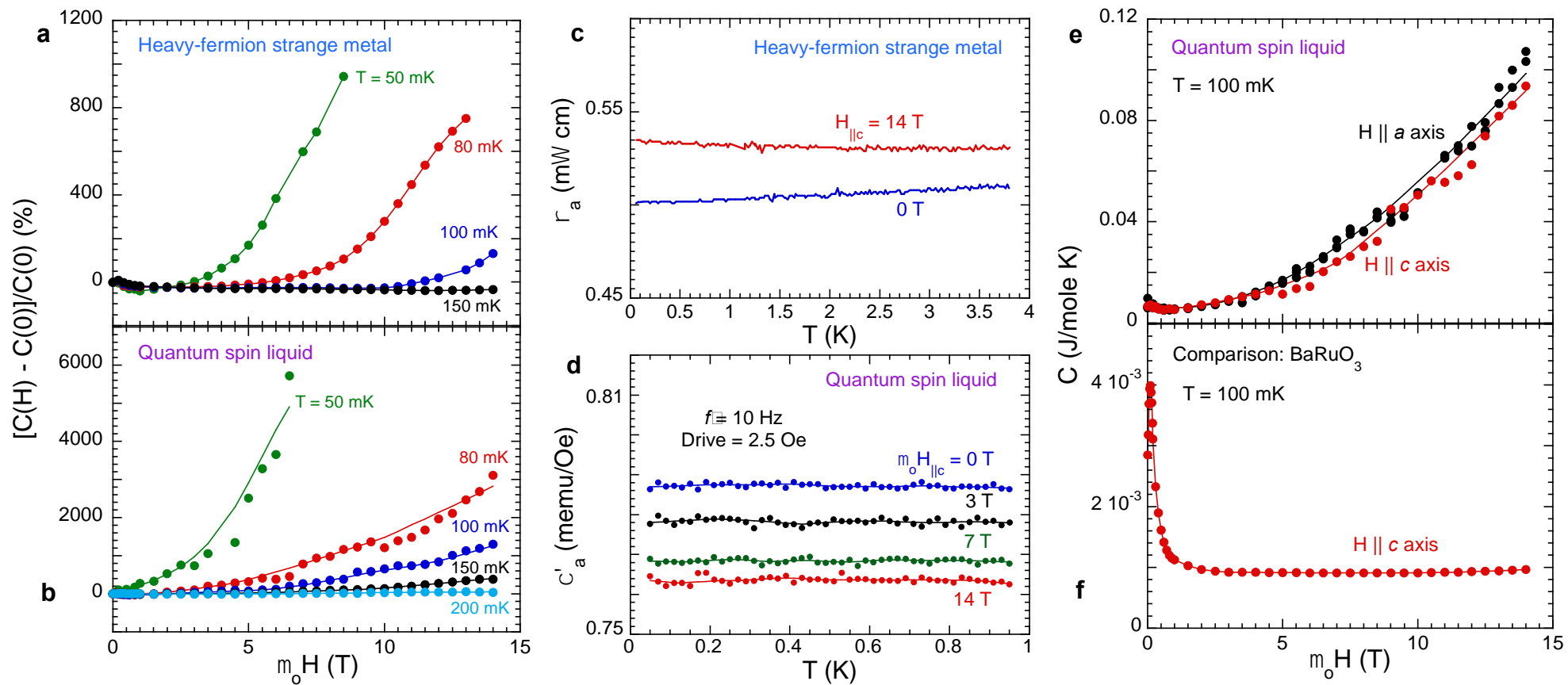


Figure 2

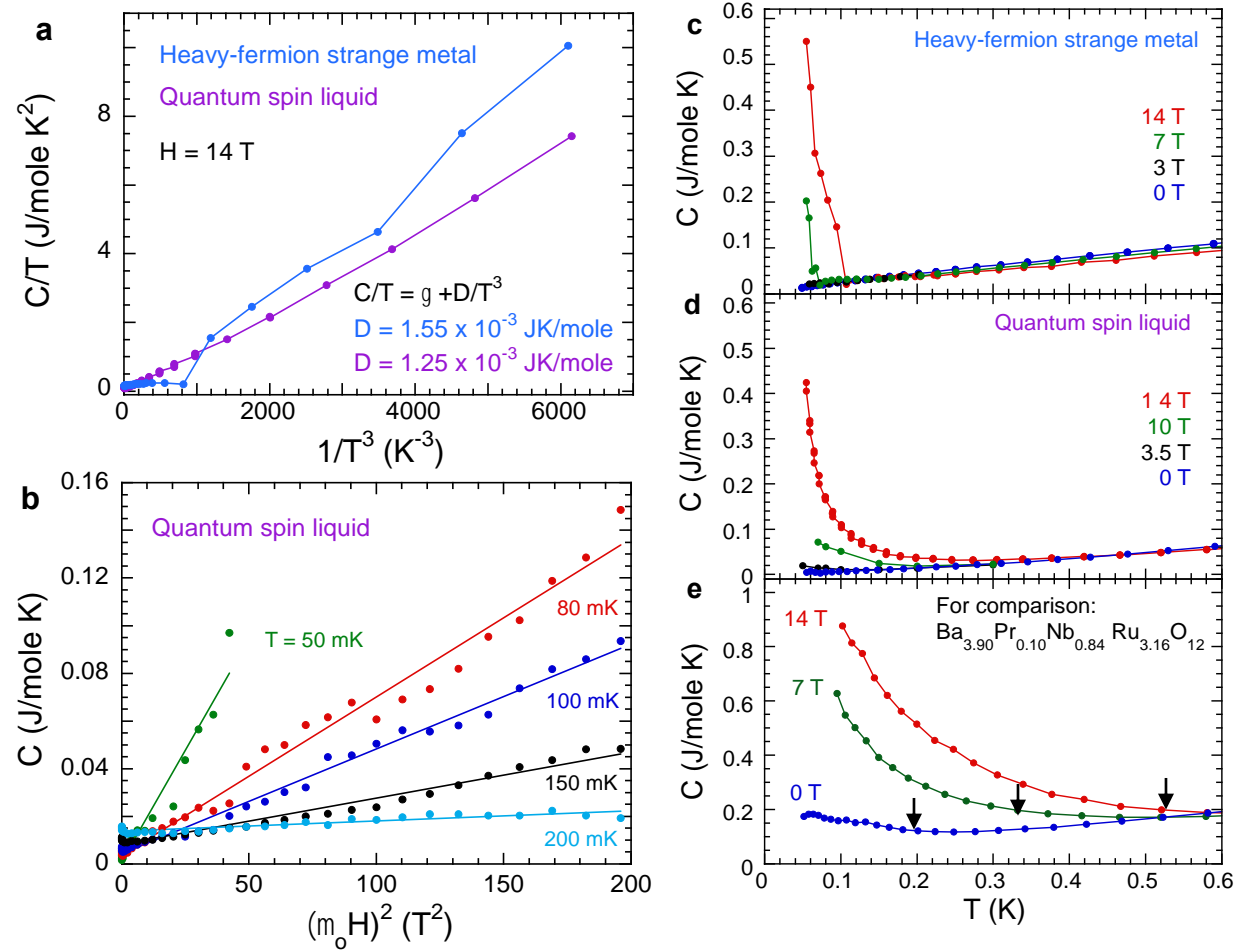


Figure 3



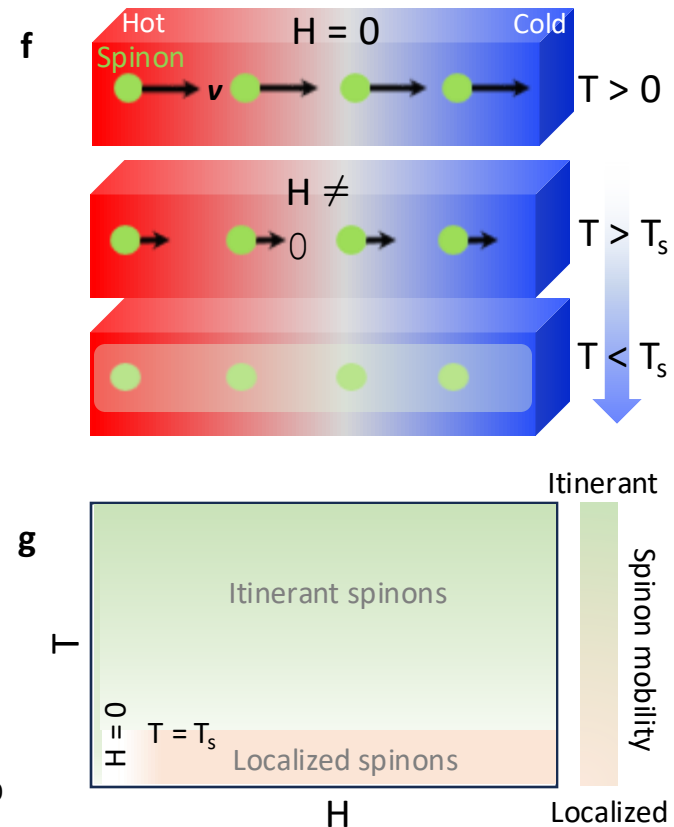
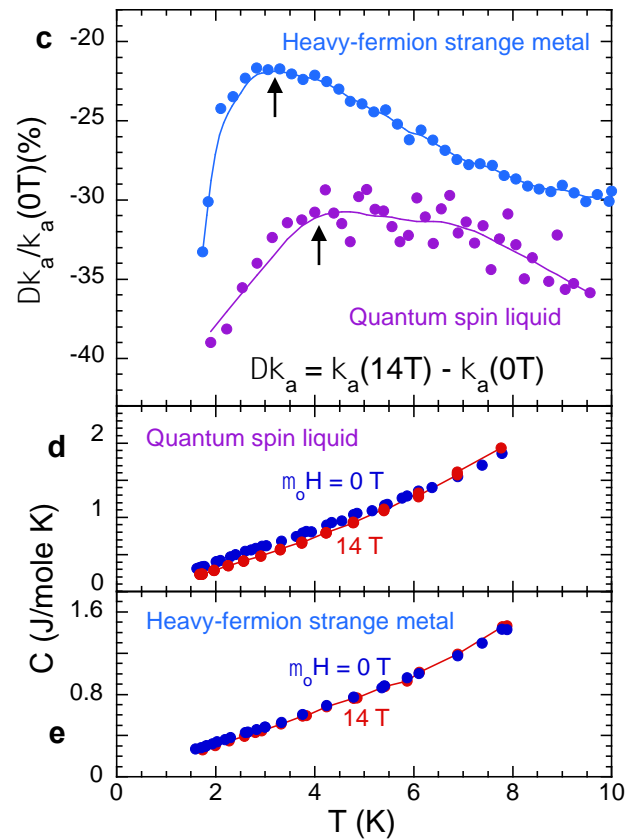
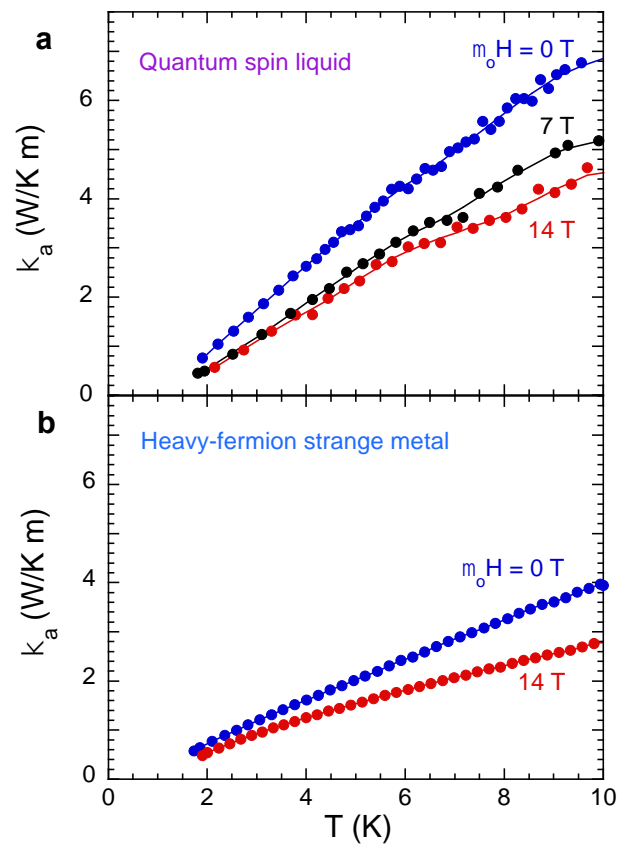


Figure 4